

Tunable Thresholds and Frequency Encoding in a Spiking NOD Controller

Ian Xul Belaustegui^a, Alessio Franci^b, Naomi Ehrich Leonard^a

Abstract—Spiking Nonlinear Opinion Dynamics (S-NOD) is an excitable decision-making model inspired by the spiking dynamics of neurons. S-NOD enables the design of agile decision-making that can rapidly switch between decision options in response to a changing environment. In S-NOD, decisions are represented by continuous time, yet discrete, opinion spikes. Here, we extend previous analysis of S-NOD and explore its potential as a nonlinear controller with a tunable balance between robustness and responsiveness. We identify and provide necessary conditions for the bifurcation that determines the onset of periodic opinion spiking. We leverage this analysis to characterize the tunability of the input-output threshold for opinion spiking as a function of the model basal sensitivity and the modulation of opinion spiking frequency as a function of input magnitude past threshold. We conclude with a discussion on S-NOD as a new neuromorphic control block and its extension to distributed spiking controllers.

I. INTRODUCTION

Decision-making, understood as the process of integrating sensory information and internal objectives to determine an agent’s actions, is a fundamental feature of virtually all biological systems and across virtually all levels of biological organization, from molecular regulatory networks [1] to neural population dynamics [2], and up to collective behaviors [3]. Modeling biological decision-making is both instrumental to understand its underlying mechanisms and to translate this understanding into engineered bio-inspired systems.

Traditional models of opinion dynamics often struggle to capture the robust yet flexible decision-making behavior observed in biological systems. The Nonlinear Opinion Dynamics (NOD) model [4], [5] shows how balancing negative and positive feedback can lead to robust, fast, and flexible decision-making through an organizing pitchfork bifurcation. However, NOD may not always be able to switch *between* decision options with sufficient agility in rapidly changing environments. The spiking-NOD (S-NOD) model [6] addresses this limitation by making NOD excitable [7]. This is achieved through adaptive slow negative feedback that brings the NOD state back to its neutral, ultra-sensitive state each time a decision is made, resulting in excitable *opinion spikes*. As an excitable system, S-NOD exhibits a form of controlled instability, where positive feedback leads to large and fast deviations away from equilibrium while slow negative feedback ensures regulation toward it. S-NOD has been applied to robot navigation in crowded environments ensuring responsiveness and indecision-breaking of the robot behavior [6]. Fig. 1 is reproduced from [6] and illustrates the agility of S-NOD as a controller.

Here, we extend the analysis in [6] to rigorously characterize the tunability of the S-NOD spiking threshold and of its input

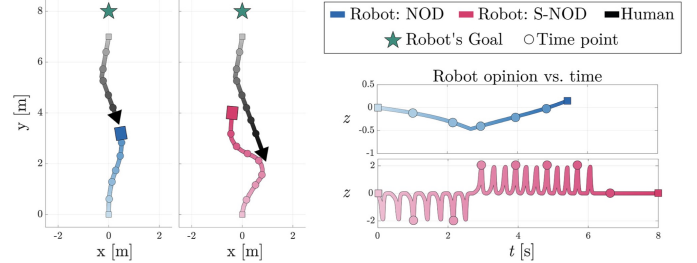


Fig. 1. Figure from [6] shows S-NOD (pink) applied to control a planar robot in a social navigation scenario. NOD (blue) is shown for comparison. The robot aims to reach a goal marked by a star while avoiding collision with an unpredictable oncoming mover (black). The NOD controller is slow to respond to an abrupt change in the direction of the oncoming mover, but the S-NOD controller responds with agility and avoids colliding.

magnitude-to-spiking frequency (fI) curve. Section II introduces S-NOD and basic facts and notation instrumental for subsequent analysis. In Section III, we study the dependence of S-NOD dynamics on the exogenous input, and prove the onset of spiking decision-making through a Hopf bifurcation occurring at an implicit, yet tunable, threshold on the input. In Section IV, we study the case where two symmetric spiking limit cycles appear in the absence of input as the model basal sensitivity is increased and the system undergoes a symmetry-breaking pitchfork bifurcation. In Section V, we study how the input spiking threshold changes and can be tuned as a function of the model basal sensitivity. Through geometric arguments, we characterize how spiking frequency increases as a function of input strength. We also discuss how the model parameters can be used to tune the shape of opinion spikes. In sum we contribute an in-depth characterization of our newly proposed S-NOD as an agile spiking control element.

II. SPIKING NONLINEAR OPINION DYNAMICS

S-NOD is governed by the differential equations

$$\begin{aligned} \dot{z} &= -d z + \tanh((k z^2 + \mu_0 - s) a z + b) \\ \dot{s} &= \varepsilon(-s + k_s z^4). \end{aligned} \quad (1)$$

The state $z(t) \in \mathbb{R}$ is the agent’s opinion at time t . For decision-making between two mutually exclusive options, we interpret $z(t) > 0$ ($z(t) < 0$) as an opinion in favor of option 1 (option 2). $|z(t)|$ is the strength of the opinion and $z(t) = 0$ is a neutral opinion (indecision). $s(t) \in \mathbb{R}$ is the agent’s slow recovery state at time t . $\mu_0 \in \mathbb{R}_+$ sets the basal level of the agent’s sensitivity¹ $\mu = k z^2 + \mu_0 - s$ to the positive feedback

¹In [6] μ , μ_0 are u , u_0 and called “attention” and “basal attention.”

term az . The agent's sensitivity μ increases with gain $k \in \mathbb{R}_+$ as the norm of the agent's opinion increases. At a much slower time-scale, μ decreases as the slow recovery variable s increases. This creates a balance of positive and negative feedback. $\varepsilon \in \mathbb{R}_+$, $\varepsilon \ll 1$ sets the timescale separation between the dynamics of z and s , so that z is fast and s is slow. $d \in \mathbb{R}_+$ is the gain of a negative feedback opinion-damping term. $a, k \in \mathbb{R}_+$ tune the positive feedback gain. $k_s \in \mathbb{R}_+$ tunes the slow negative feedback gain. $b \in \mathbb{R}$ is an exogenous input. In applications b would integrate various task-relevant signals, and represent evidence for a decision in the positive or negative z direction.

Here we establish some basic results needed to analyze the onset of opinion spiking as either b (in Section III) or μ_0 increases (in Section IV).

Remark II.1. *The fixed points of equation (1) have the form $(\hat{z}, k_s \hat{z}^4)$, where \hat{z} solves the equation*

$$h(\hat{z}) := -d\hat{z} + \tanh(a\hat{z}(-k_s\hat{z}^4 + k\hat{z}^2 + \mu_0) + b) = 0. \quad (2)$$

The stability of equilibria of two-dimensional systems is fully determined by the trace and determinant of the Jacobian evaluated at equilibrium. Let $\varphi(z, s) := az(kz^2 + \mu_0 - s) + b$, $\psi(z) := \varphi(k_s z^4, z) = az(-k_s z^4 + kz^2 + \mu_0) + b$, and $f(z, s) := (\dot{z}, \dot{s})$. The Jacobian of (1) is

$$J(z, s) := D_{(z,s)}f(z, s) \quad (3)$$

$$= \begin{pmatrix} -d + \tanh'(\varphi(z, s)) \frac{\partial \varphi}{\partial z} & \tanh'(\varphi(z, s)) \frac{\partial \varphi}{\partial s} \\ 4\varepsilon k_s z^3 & -\varepsilon \end{pmatrix},$$

where $\tanh'(x) = 1 - \tanh^2(x)$.

Remark II.2. *At a fixed point $(\hat{z}, k_s \hat{z}^4)$, we have that $\tanh'(\varphi(\hat{z}, k_s \hat{z}^4)) = 1 - d^2 \hat{z}^2$.*

Let $J_{\hat{z}} := J(\hat{z}, k_s \hat{z}^4)$.

Lemma II.3. *If $(\hat{z}, k_s \hat{z}^4)$ is a fixed point for (1), then*

$$\text{tr } J_{\hat{z}} = \underbrace{ad^2 k_s}_{c_3} \hat{z}^6 - \underbrace{(3ad^2 k + ak_s)}_{c_2} \hat{z}^4 + \underbrace{(3ak - ad^2 \mu_0)}_{c_1} \hat{z}^2 + \underbrace{a\mu_0 - d - \varepsilon}_{c_0} \quad (4)$$

$$\frac{\det J_{\hat{z}}}{\varepsilon} = -\underbrace{5ad^2 k_s}_{\hat{c}_3=5c_3} \hat{z}^6 + \underbrace{(3ad^2 k + 5ak_s)}_{\hat{c}_2=c_2+4ak_s} \hat{z}^4 - \underbrace{(3ak - ad^2 \mu_0)}_{\hat{c}_1=c_1} \hat{z}^2 - \underbrace{(a\mu_0 - d)}_{\hat{c}_0=c_0}. \quad (5)$$

The proof follows from elementary algebraic manipulations and is omitted. Finding the roots of these polynomials reduces to solving two third-degree polynomials. Also, if $(\hat{z}, k_s \hat{z}^4)$ is a fixed point, then

$$h'(\hat{z}) = -d + (1 - d^2 \hat{z}^2) \psi'(\hat{z}) = -\frac{\det J_{\hat{z}}}{\varepsilon}. \quad (6)$$

We use this expression to bound the number of fixed points.

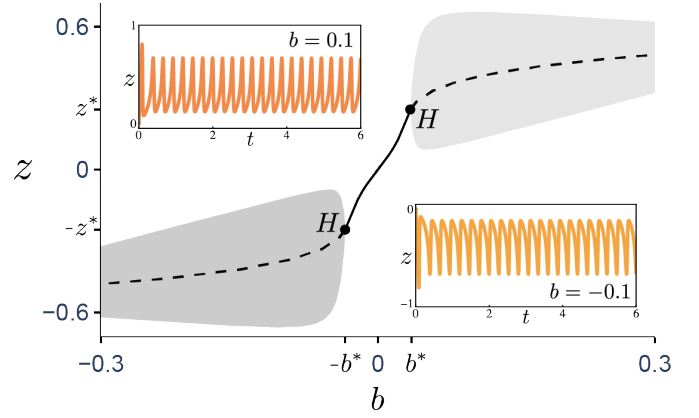


Fig. 2. Bifurcation diagram for (1) with respect to input (b) projected onto the opinion (z) axis to reduce from three dimensions to two. Solid lines indicate stable nodes, dashed lines indicate unstable nodes, shaded areas indicate stable limit cycles, vertical width of shaded area represents amplitude of spike. Dots marked with H correspond to the Hopf bifurcations at $\pm b^*$. Inset plots show dynamics for suprathreshold positive ($b = 0.1$) and negative ($b = -0.1$) input leading to spikes. Parameters used are $\mu_0 = 0.8$, $a = 1$, $d = 1$, $k = 2.3$, $k_s = 16$, $\varepsilon = 0.1$.

III. SPIKING FROM INCREASING b

For certain conditions on parameters we can prove the system undergoes a Hopf bifurcation with respect to the input b at a critical input threshold $\pm b^*$, after which the system goes from a resting state to spiking. Fig. 2 shows a bifurcation diagram projected onto the opinion axis, showing the stability of fixed points and amplitude of the spike limit cycle, as well as two symmetric examples of spiking. All the analysis in this section is presented for $b \geq 0$, since the case $b \leq 0$ follows directly from symmetry.

A Hopf bifurcation is characterized by a fixed point having a pair of conjugate non-zero purely imaginary eigenvalues crossing the imaginary axis as a bifurcation parameter passes a critical value. This gives us a useful characterization of the first condition needed to identify a Hopf bifurcation.

Remark III.1. *A fixed point $(\hat{z}, k_s \hat{z}^4)$ for (1) has two conjugate, purely imaginary, non-zero eigenvalues if and only if $\text{tr } J_{\hat{z}} = 0$ and $\det J_{\hat{z}} > 0$.*

Since our approach is implicit, we first consider the situation where the fixed point is unique for all inputs. Let $\zeta_0 = \frac{\hat{c}_2 - \sqrt{\hat{c}_2^2 - 3\hat{c}_1\hat{c}_3}}{3\hat{c}_3}$. The following result provides a tight sufficient condition for the uniqueness of the fixed point.

Proposition III.2. *If $\zeta_0 \in \mathbb{R}_+$ and $\det J_{\sqrt{\zeta_0}} > 0$, then for all $b \in \mathbb{R}$ there is a unique fixed point of (1).*

Proof. Let $b \geq 0$. We first show that there is at least one fixed point. If $b = 0$ then $h(0) = 0$. Otherwise, if $b > 0$ then $h(0) = \tanh(b) > 0$, and $\lim_{z \rightarrow \infty} h(z) = -\infty$, which by continuity implies there is a point $\hat{z} > 0$ such that $h(\hat{z}) = 0$. In either case there is a fixed point for (1).

Equation (1) for \dot{z} implies that any fixed point $(\hat{z}, k_s \hat{z}^4)$ must satisfy $\hat{z} \in [-d^{-1}, d^{-1}]$.

We now show that $\forall z \in [0, d^{-1}], h(z) = 0 \Rightarrow h'(z) < 0$, which implies there can be at most one root for h in $[0, d^{-1}]$, since consecutive roots can't both have strictly negative derivative. From (6) we have $h(z) = 0 \Rightarrow h'(z) = -\frac{\det J_z}{\varepsilon}$. Consider the third degree polynomial $q_{det}(z) := -\frac{\det J_z}{\varepsilon} = \hat{c}_3 z^3 - \hat{c}_2 z^2 + \hat{c}_1 z + c_0$. From (6) it follows that $q_{det}(d^{-2}) = -\det J_{d^{-1}}/\varepsilon = -d < 0$, and since $\hat{c}_3 > 0$, then $\lim_{z \rightarrow \infty} q_{det}(z) = \infty$. So there is a root of q_{det} greater than d^{-2} . The two inflection points of q_{det} are given by $\zeta_0 = \frac{\hat{c}_2 - \sqrt{\hat{c}_2^2 - 3\hat{c}_1\hat{c}_3}}{3\hat{c}_3}$ and $\zeta_1 = \frac{\hat{c}_2 + \sqrt{\hat{c}_2^2 - 3\hat{c}_1\hat{c}_3}}{3\hat{c}_3}$. Since we assume $\zeta_0 \in \mathbb{R}_+$, we have $\zeta_0 \leq \zeta_1$ and $q_{det}(\zeta_0) \geq q_{det}(\zeta_1)$. Thus, if $q_{det}(\zeta_0) < 0$ then $\forall z \in [0, d^{-2}], q_{det}(z) < 0$. But $q_{det}(\zeta_0) = -\frac{\det J_{\zeta_0}}{\varepsilon} < 0$ by hypothesis. So we conclude $\forall z \in [0, d^{-1}], -\det J_z < 0$, which implies there is a unique root for h , and so a unique fixed point for (1). \square

In general, for sufficiently small μ_0 the fixed point is unique. The next proposition tells us that this point is increasing with respect to b .

Proposition III.3. *Let $\zeta_0 \in \mathbb{R}_+$, $\det J_{\sqrt{\zeta_0}} > 0$. Let $\hat{z}_b \in \mathbb{R}$ be the unique zero of h for a given $b \in \mathbb{R}$. Then $\lim_{b \rightarrow \infty} \hat{z}_b = d^{-1}$ and \hat{z}_b is a strictly increasing function of b .*

Proof. $\forall z \in \mathbb{R}, \lim_{b \rightarrow \infty} \psi(z) = \infty$, which implies

$$\begin{aligned} \lim_{b \rightarrow \infty} h(z) &= \lim_{b \rightarrow \infty} (-dz + \tanh(\psi(z))) \\ &= -dz + \lim_{b \rightarrow \infty} (\tanh(\psi(z))) = -dz + 1. \end{aligned}$$

From this it follows that \hat{z}_b converges to the unique zero of $-dz + 1$, namely $\lim_{b \rightarrow \infty} \hat{z}_b = d^{-1}$.

From the proof of Prop. III.2 it follows that $\det J_{\sqrt{\zeta_0}} > 0$ implies $\forall z \in [0, d^{-1}], \det J_z > 0$. Taking implicit derivatives of the relation $h(\hat{z}) = 0$:

$$\begin{aligned} 0 &= -d \frac{\partial \hat{z}_b}{\partial b} + \tanh'(\psi(\hat{z}_b)) \frac{\partial \psi}{\partial b}(\hat{z}_b) \\ &= -d \frac{\partial \hat{z}_b}{\partial b} + (1 - d^2 \hat{z}_b^2) (1 + \psi'_b(\hat{z}_b) \frac{\partial \hat{z}_b}{\partial b}) \\ \Rightarrow \frac{\partial \hat{z}_b}{\partial b} &= \frac{1 - d^2 \hat{z}_b^2}{d - (1 - d^2 \hat{z}_b^2) \psi'_b(\hat{z}_b)} = \frac{\varepsilon(1 - d^2 \hat{z}_b^2)}{\det J_{\hat{z}_b}}, \end{aligned}$$

where the last equality comes from (6). Since $\hat{z}_b \in [0, d^{-1}]$ and $\det J_{\hat{z}_b} > 0$, we conclude that $\forall b \in \mathbb{R}_+, \frac{\partial \hat{z}_b}{\partial b} > 0$. \square

The previous result holds in general for how the fixed point at the origin varies with b , although in the case where the fixed point is not unique the continuation of the origin might cease to exist in a saddle node bifurcation. Now, let $\xi_0 = \frac{c_2 - \sqrt{c_2^2 - 3c_1c_3}}{3c_3}$. The following proposition tells us about the trace of the Jacobian at the fixed point when $\mu_0 < \frac{d}{a}$ but not too small, $k > \frac{d^3}{3a}$ and $\varepsilon > 0$ small enough.

Proposition III.4. *If $c_0 - \varepsilon < 0$, $\xi_0 \in \mathbb{R}_+$ and $\text{tr } J_{\sqrt{\xi_0}} > 0$, there exist $z^*, z^{**} \in [0, d^{-1}]$ such that $\text{tr } J_{z^*} = \text{tr } J_{z^{**}} = 0$ and $\forall z \in [0, z^*) \cup (z^{**}, d^{-1}], \text{tr } J_z < 0$, and $\forall z \in (z^*, z^{**}), \text{tr } J_z > 0$.*

Proof. ξ_0 and $\xi_1 := \frac{c_2 + \sqrt{c_2^2 - 3c_1c_3}}{3c_3} \geq \xi_0$ are the two inflection points of the polynomial $q_{tr}(z) = \text{tr } J_{\sqrt{z}} = c_3 z^3 - c_2 z^2 + c_1 z + c_0 - \varepsilon$. We also have $\lim_{z \rightarrow \infty} q_{tr}(z) = \infty$, $\lim_{z \rightarrow -\infty} q_{tr}(z) = -\infty$, $q_{tr}(0) = c_0 - \varepsilon < 0$ and $q_{tr}(d^{-2}) = -d - \varepsilon < 0$. Thus, $\max_{z \in [0, d^{-2}]} q_{tr}(z) = q_{tr}(\xi_0) = \text{tr } J_{\sqrt{\xi_0}} > 0$. Since $\text{tr } J_z = q_{tr}(z^2)$, this implies that for $\text{tr } J_z$ there exist two roots $z^*, z^{**} \in [0, d^{-1}]$, $z^* < z^{**}$, which satisfy the desired properties. \square

The following theorem describes the bifurcations with respect to b .

Theorem III.5 (Spiking Input Threshold).

Suppose $\zeta_0, \xi_0 \in \mathbb{R}_+$, $\det J_{\sqrt{\zeta_0}} > 0$ and $\text{tr } J_{\sqrt{\xi_0}} > 0$. Then there exist exactly two critical values of input $b^, b^{**} \in \mathbb{R}_+$ at which the unique fixed point undergoes a Hopf bifurcation (and symmetrically for negative values of the input).*

Proof. From the proof of Prop. III.2 it follows that $\det J_{\sqrt{\zeta_0}} > 0$ implies $\forall z \in [0, d^{-1}], \det J_z > 0$. In particular $\det J_0 = -\varepsilon c_0 > 0$, so for any $\varepsilon > 0$ we have $c_0 - \varepsilon < 0$. Thus, by Prop. III.4 there exist $z^*, z^{**} \in [0, d^{-1}]$ roots of $\text{tr } J_z$ as in the statement. We have $\hat{z}_0 = 0$, and by Prop. III.3 we know $\lim_{b \rightarrow \infty} \hat{z}_b = d^{-1}$. So by continuity there exist $b^*, b^{**} \in \mathbb{R}_+$ such that $\hat{z}_{b^*} = z^*$ and $\hat{z}_{b^{**}} = z^{**}$. Thus $\text{tr } J_{\hat{z}_{b^*}} = \text{tr } J_{\hat{z}_{b^{**}}} = 0$ and $\det J_{\hat{z}_{b^*}} > 0$ and $\text{tr } J_{\hat{z}_{b^{**}}} > 0$. By Remark III.1 at these two values of b the fixed point has two non-zero conjugate purely imaginary eigenvalues.

Transversality follows from the fact that \hat{z}_b is strictly increasing with respect to b , which also implies uniqueness of critical values b^* and b^{**} . By Thm. 3.4.2 in [8] we conclude that at $b = b^*$ the unique fixed point goes from being a stable node to an unstable source in a Hopf bifurcation, and at $b = b^{**}$ it goes from being an unstable source to a stable node, also in a Hopf bifurcation. \square

The threshold to spiking at b^* can be expressed as the solution to the implicit equation $-dz^* + \tanh((-k_s z^{*4} + k z^{*2} + \mu_0) a z^* + b^*) = 0$, where z^* can be written in closed form as the solution to a third degree polynomial. Even though from the previous analysis we cannot conclude whether the Hopf bifurcations in Thm. III.5 are supercritical or subcritical, we have the following result, which guarantees the existence of a limit cycle precisely in the interval after the first Hopf and before the second.

Theorem III.6 (Limit Cycle After Input Threshold).

If $\zeta_0, \xi_0 \in \mathbb{R}_+$, $\det J_{\sqrt{\zeta_0}} > 0$ and $\text{tr } J_{\sqrt{\xi_0}} > 0$, then for input values $b \in (b^, b^{**})$ there exists a limit cycle.*

Proof. First, $b \in (b^*, b^{**}) \Rightarrow \hat{z}_b \in (z^*, z^{**}) \Rightarrow \text{tr } J_{\hat{z}_b} > 0$, which together with $\det J_{\hat{z}_b} > 0$ implies the unique fixed point is unstable. Next, we show the dynamics of the system are bounded. Let the bounding box be $\mathcal{B} = [-d^{-1}, d^{-1}] \times [-1, k_s d^{-4}]$. We consider in turn the four edges of the box to show that no trajectory starting in the box escapes it. First, suppose $(z, s) \in (-d^{-1}, d^{-1}) \times \{-1\}$, then $\dot{s} = -s + k_s z^4 = 1 + k_s z^4 > 1 > 0$, so the vector field points towards the inside

of the box along this edge. If $(z, s) \in (-d^{-1}, d^{-1}) \times \{k_s d^{-4}\}$ then $\dot{s} = -k_s d^{-4} + k_s z^4 = k_s(z^4 - \frac{1}{d^4}) < k_s(\frac{1}{d^4} - \frac{1}{d^4}) = 0$, and so the vector field points towards the inside of the box along this edge as well. Considering the top edge, if $(z, s) \in \{d^{-1}\} \times (-1, k_s d^{-4})$ then $\dot{z} = -dz + \tanh(\psi(z)) < -1 + 1 = 0$, so the field points down into the box. Now for the bottom edge, if $(z, s) \in \{-d^{-1}\} \times (-1, k_s d^{-4})$, we get symmetrically that $\dot{z} = -dz + \tanh(\psi(z)) > 1 - 1 = 0$, and so the field points up into the box. Finally, if we consider the four corner points: if $s = -1, z = d^{-1}$ then $\dot{s} > 0, z < 0$; if $s = -1, z = -d^{-1}$ then $\dot{s} > 0, z > 0$; if $s = k_s d^{-4}, z = d^{-1}$ then $\dot{s} = 0, z < 0$; and if $s = k_s d^{-4}, z = -d^{-1}$ then $\dot{s} = 0, z > 0$. This all follows from the previous observations and implies that all orbits starting on the boundary of \mathcal{B} stay in \mathcal{B} . Noting that $\hat{z}_b \in \mathcal{B}$ is an unstable source and there are no other fixed points, we can apply the Poincaré-Bendixson theorem [8] to conclude that there exists a limit cycle in \mathcal{B} and that every trajectory converges to a limit cycle. \square

The next proposition covers the case when there is no input threshold, that is, when there is always only a stable fixed point for all $b \in \mathbb{R}$ and there is no spiking. This case always happens for μ_0 small enough.

Proposition III.7. *Suppose $\zeta_0, \xi_0 \in \mathbb{R}_+$, $\det J_{\sqrt{\zeta_0}} > 0$ and $\text{tr } J_{\sqrt{\xi_0}} < 0$. Then for all $b \in \mathbb{R}$ the unique fixed point of equation 1 is stable.*

Proof. From the proof of Prop. III.4 follows that if $\text{tr } J_{\sqrt{\xi_0}} < 0$ then $\forall z \in [0, d^{-1}]$, $\text{tr } J_z < 0$, which together with $\det J_z > 0$ implies stability. \square

The case where $\zeta_0, \xi_0 \in \mathbb{R}_+$, $c_0 < 0$ and $\text{tr } J_{\sqrt{\xi_0}} > 0$ but $\det J_{\sqrt{\zeta_0}} < 0$ (when $c_0 = a\mu_0 - d$ is slightly less than 0) turns out to be equivalent in its behavior to that described in Thm. III.5, but presents some additional subtleties in its analysis. In summary, the fixed point can no longer be shown to be unique but the behavior is identical, with either the same Hopf at b^* or a saddle-node annihilation acting as the input threshold to spiking.

The remaining case of $c_0 > 0$ corresponds to the origin being a saddle point for no input, and is discussed next.

IV. SPIKING ONSET BY INCREASING μ_0 WHEN $b = 0$

We consider the case where the input is fixed at $b = 0$ and study the bifurcation that happens with respect to μ_0 at the critical point $\mu_0^* = \frac{d}{a}$. Locally at the origin this bifurcation is a subcritical pitchfork as shown in Fig. 3. This can be shown by projecting the local dynamics around the origin, which reduces to the single-agent non-excitable fast and flexible nonlinear opinion dynamics [5].

Globally, we have that for critical and supercritical values of μ_0 there exist exactly three fixed points, one of which is the origin. The other two are symmetric with respect to the horizontal $z = 0$, and their properties determine the global behavior of the system. We prove conditions under which the two other fixed points at the critical μ_0 are source nodes, which ensures that for some open interval beyond μ_0^* the system has

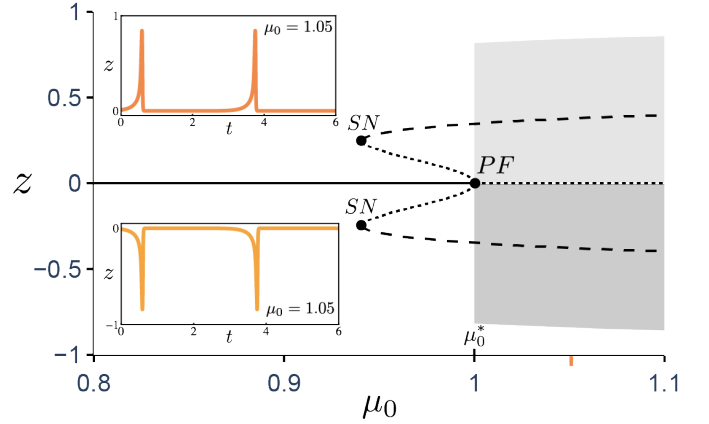


Fig. 3. Bifurcation diagram of system (1) with respect to basal sensitivity (μ_0) projected onto the opinion state (z) axis to reduce from three dimensions to two. Solid lines indicate stable nodes, dashed lines indicate unstable nodes, dotted lines indicate saddle points, shaded areas indicate the two stable limit cycles in different shades of gray. The vertical width of shaded areas represent amplitude of spike. Black dots represent bifurcations, one subcritical pitchfork (PF) and two symmetric saddle-node bifurcations (SN). Inset figures show positive (top, $z(0) = 0.1$) and negative (bottom, $z(0) = -0.1$) spike limit cycles for $\mu_0 = 1.05$. Parameters used are $b = 0, a = 1, d = 1, k = 2.3, k_s = 16, \varepsilon = 0.1$.

two symmetric limit cycles, each of which encircles one of the nonzero fixed points. These two large amplitude limit cycles correspond to spikes that emerge in a qualitatively different way than in the previous section. They do not appear through a Hopf bifurcation but through the breaking off of homoclinic orbits at the subcritical pitchfork. Fig. 3 shows a representative bifurcation diagram projected onto the opinion subspace.

First, observe that the stability of the origin changes at μ_0^* : when $\mu_0 < \frac{d}{a}$ then $c_0 = \mu_0 a - d < 0$ so $\det J_0 > 0$ and $\text{tr } J_0 < 0$, which implies the fixed point at the origin is a stable node. When $\mu_0 > \frac{d}{a}$ we have $\mu_0 a - d > 0$ so $\det J_0 < 0$, which implies the fixed point is a saddle point. When $b = 0$ the horizontal line $z = 0$ is invariant and is actually part of the stable manifold of the fixed point in the origin. Thus, we have the following.

Proposition IV.1. *For any parameters with $b = 0$ there are no limit cycles encircling the origin. If the parameters are such that the origin is the only fixed point, then there are no limit cycles.*

Proof. Suppose $b = 0$, then the origin is a fixed point and the horizontal $z = 0$ is invariant. If there existed a limit cycle surrounding the origin it would intersect the horizontal, but this leads to a contradiction.

Suppose the parameters are chosen such that the origin is the only fixed point and there exists a limit cycle. This limit cycle cannot encircle the origin. Then index theory tells us that there must be some other fixed point encircled by the limit cycle, which is a contradiction. \square

Now we will show that for supercritical values of μ_0 the system has exactly three fixed points.

Proposition IV.2. *If $\mu_0 \geq \frac{d}{a}$ and $k > \frac{d^3}{3a}$ then (2) has exactly three solutions.*

Proof. First, $h(0) = 0$ implies $(0, 0)$ is a fixed point. The Taylor expansion of h has terms $h(z) = (a\mu_0 - d)z + a(k - \frac{a^2\mu_0^3}{3})z^3 + \mathcal{O}(z^5)$. So $h'(0) = a\mu_0 - d \geq 0$, $h''(0) = 0$, $h'''(0) = 6a(k - \frac{a^2\mu_0^3}{3}) > 0$. This implies the function is monotonically increasing for some open interval after zero. Observe also that $\lim_{z \rightarrow \infty} h(z) = -\infty$, so there must be at least one fixed point greater than zero.

To show that there are no more than three solutions recall the remark that for any fixed point which solves $h(\hat{z}) = 0$ we have $h'(\hat{z}) = -\varepsilon^{-1} \det J_{\hat{z}}$. Considering this as a third degree polynomial with respect to \hat{z}^2 , there can be at most three positive solutions. However, by hypothesis $-\varepsilon^{-1} \det J_0 = a\mu_0 - d \geq 0$, and from (6) $-\varepsilon^{-1} \det J_{d^{-1}} = -d < 0$. Thus, there is exactly one root for $\det J_z$ in the interval $(0, d^{-1})$, denoted by $\rho_0 \in (0, d^{-1})$, and it satisfies that $\forall z^2 \in (0, \rho_0)$, $-\varepsilon^{-1} \det J_z > 0$, and $\forall z^2 \in (\rho_0, 1/d)$, $-\varepsilon^{-1} \det J_z < 0$. Using symmetry and the fact that there can be no solution greater than d^{-1} , we conclude there are exactly three solutions. \square

To prove the existence of limit cycles for $\mu_0 > \mu_0^*$ we again make use of the Poincaré-Bendixon theorem, which tells us that a compact subset of the plane that is forward invariant and contains only a hyperbolic source must also contain a limit cycle. We give a sufficient condition for this.

Theorem IV.3 (Spike Limit Cycles After Critical μ_0).

If $\frac{d^3}{3a} < k < k_s \frac{c_2 - \sqrt{c_2^2 - 4c_1c_3}}{2c_3}$ then for sufficiently small $\varepsilon > 0$ there exists $\tau > 0$ such that for $\mu_0 \in (\mu_0^, \mu_0^* + \tau)$ there exist two symmetric limit cycles, each of which encircles one of the two fixed points that are not the origin and every trajectory converges to some limit cycle.*

Proof. First we show that the fixed point is unstable at $\mu_0 = \mu_0^*$. The value $\sqrt{k/k_s}$ is the positive root of the polynomial $-dz + \psi(z)$, which given the assumptions has exactly three roots. The polynomial $\psi(z)$ also has exactly three roots. Let $\varsigma \in (0, d^{-1})$ denote its positive root. Since $x > 0 \Rightarrow \tanh(x) < x$, then $\forall z \in (0, \varsigma)$, $h(z) < -dz + \psi(z)$. Thus $-dz + \psi(z)$ is an over-estimator this interval, and so the unique positive root $\hat{z} \in (0, d^{-1})$ of $h(z)$ is smaller than $\sqrt{k/k_s}$. At the limit $\varepsilon = 0$, using what we know of $\text{tr } J_z$ from previous analysis and the fact that $k > \frac{d^3}{3a}$ implies $c_1 > 0$, we have that $\text{tr } J_z$ has exactly one root at the point $\varrho = \sqrt{\frac{c_2 - \sqrt{c_2^2 - 4c_1c_3}}{2c_3}} \in (0, d^{-1})$, and $\forall z \in (0, \varrho)$, $\text{tr } J_z > 0$. Since by hypothesis $\sqrt{k/k_s} < \varrho$, we conclude for $\varepsilon > 0$ small enough $\text{tr } J_{\hat{z}} > 0$. Since $-\varepsilon^{-1} \det J_z$ is positive between 0 and its first positive root, it must be the case also that $\det J_{\hat{z}} > 0$, since otherwise $\hat{z} = \int_{t=0}^{\hat{z}} h'(t)dt < 0$ which is a contradiction. Thus, we conclude that \hat{z} is an unstable source, and it is unstable for some open interval above μ_0^* .

To construct a bounding region in the positive opinion half-space (symmetrically for the negative) we use the following

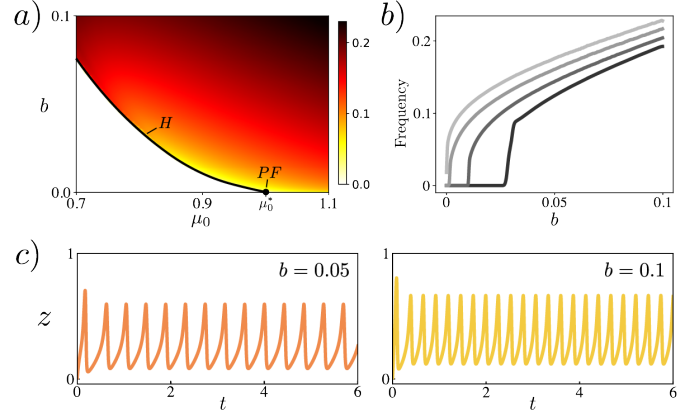


Fig. 4. **a)** Region of the (μ_0, b) parameter space. For each point, color represents the frequency of spiking obtained through numerical analysis. Black line marked with H represents Hopf bifurcation and point marked with PF is the subcritical pitchfork bifurcation. Only a section of the positive opinion halfspace is shown to save space, since the negative halfspace is the symmetric reflection along the horizontal axis. **b)** Comparison of four vertical slices of **a)** for values of μ_0 equal to 0.82, 0.9, 0.98, and 1.06 in order of decreasing shade of gray. **c)** Spiking for two values of b corresponding to those in Fig. 5 and $\mu_0 = 0.8$. For all subfigures parameters are $a = 1$, $d = 1$, $k = 2.3$, $k_s = 16$, $\varepsilon = 0.1$.

construction for the boundary. First take the line segment from point $(d^{-1}, -1) \in \mathbb{R}^2$ to $(d^{-1}, k_s d^{-4})$. Then run a line down from $(d^{-1}, k_s d^{-4})$ to a point $(\varpi, k_s d^{-4})$ such that when continuing the orbit from that point it first crosses the line $s = \mu_0 - \mu_0^*$ at a point $(\tilde{\omega}, \mu_0 - \mu_0^*)$ such that $\dot{z} > 0$ and $\tilde{\omega} < \hat{z}$. This is possible because the horizontal $z = 0$ is the stable manifold of the origin, so it is possible to take a point close enough to pass as close as desired to the origin, and so to cross the vertical $s = \mu_0 - \mu_0^*$ as close as desired to the horizontal axis as well. Since the first terms of the Taylor expansion of \dot{z} restricted to that line is $\dot{z}(\mu_0 - \mu_0^*, z) = (ak - \frac{d^3}{3})z^3 + \mathcal{O}(z^5)$, then there is a neighborhood above $(0, \mu_0 - \mu_0^*)$ where $\dot{z} > 0$. We include the trajectory from $(\varpi, k_s d^{-4})$ to $(\tilde{\omega}, \mu_0 - \mu_0^*)$ as part of the bottom boundary of our region. Then, we include also the line from $(\tilde{\omega}, \mu_0 - \mu_0^*)$ to $(\tilde{\omega}, -1)$ also into the bottom side. Finally, we close the region by including the line segment from $(\tilde{\omega}, -1)$ to $(d^{-1}, -1)$ as the left boundary. This region contains the fixed point by construction, and the vector field along the boundary can be seen to point inward. Thus, we can apply the Poincaré-Bendixon theorem to conclude that there exists a limit cycle and that every trajectory converges to a limit cycle. \square

The resulting limit cycles appear through global bifurcations of two homoclinic orbits to the origin at $\mu_0 = \mu_0^*$. This implies that close to the critical μ_0^* the limit cycles have arbitrarily small frequency. This is a desirable property, since it implies that while in the slightly supercritical μ_0 regime even very small noise can lead to spiking, this will be at a low frequency such that it will just have the effect of breaking symmetry but will not make the system overly sensitive to noise.

V. TUNABILITY OF INPUT THRESHOLD AND FREQUENCY ENCODING

In the previous two sections we rigorously showed the identity of the bifurcations that happen at the onset of spiking in the S-NOD system. These happen through two routes. One is through a Hopf bifurcation for supra-threshold inputs at fixed values of μ_0 , which leads to the rapid appearance of a single spike limit cycle in either the positive or negative opinion halfspaces, depending on the sign of the input. The other is through a pitchfork bifurcation that happens at the origin when there is no input and the parameter μ_0 crosses the critical value μ_0^* . Representative bifurcation diagrams of these two routes are shown in Figs. 2 and 3 respectively. A fuller picture can be obtained by considering both parameters simultaneously, as shown in Fig. 4a, where the input threshold as well as its dependence on μ_0 can be observed. In the figure, the area in white corresponds to the situation of a single (globally) stable fixed point, whereas the colored region corresponds to a single (globally) attracting spike limit cycle. The input threshold decreases with increasing μ_0 , until it completely vanishes at μ_0^* . This figure also suggests that the pitchfork bifurcation route is rather special, in the sense that most trajectories along the (μ_0, b) parameter space going from the resting to spiking regions pass through a Hopf bifurcation. In this sense the Hopf route is the generic one. Fig. 4a also shows the dependence of the input threshold b^* on the parameter μ_0 . As μ_0 increases b^* becomes smaller.

Proposition V.1. *For $\mu_0 < \mu_0^*$ such that the input threshold b^* exists and for sufficiently small $\varepsilon > 0$, the input threshold is decreasing with respect to μ_0 , i.e. $\frac{\partial b^*}{\partial \mu_0} < 0$.*

Proof. From equation 2 it follows by implicit differentiation that $\frac{\partial b^*}{\partial \mu_0} = \frac{\det J_{z^*}}{1-d^2 z^{*2}} \frac{\partial z^*}{\partial \mu_0}$, where z^* is as in Prop. III.4. By comparing polynomials $\text{tr } J_z$ and $\det J_z$ it can be seen that $\forall z \in (-d^{-1}, d^{-1}), -\varepsilon^{-1} \det J_z < \text{tr } J_z$ for sufficiently small $\varepsilon > 0$, thus $\frac{\det J_{z^*}}{1-d^2 z^{*2}} > 0$. Then, $\frac{\partial \text{tr } J_z}{\partial \mu_0} = a(1-d^2 z^2)$ implies $\frac{\partial z^*}{\partial \mu_0} < 0$. Thus, $\frac{\partial b^*}{\partial \mu_0} < 0$. \square

S-NOD also displays encoding of the input magnitude as the spiking frequency, which can be observed both in Fig. 4a as the color intensity in the spiking region and also in Fig. 4b where four ‘‘slices’’ are taken for fixed values of μ_0 . For fixed values of μ_0 , the frequency is always an increasing function of the input, within the range shown. Proving this fact analytically is not trivial, but can be understood through a geometric understanding of how the system nullclines vary with the input. For a fixed value of $z \in (0, d^{-1})$, there is a unique solution to the \dot{z} equation in (1) for $s \in \mathbb{R}$. The way this solution varies with b is linear with slope $(az)^{-1}$. Thus, for values of z closer to d^{-1} the rate of change of the z nullcline increases. Since we consider $\varepsilon > 0$ very small, the spike limit cycle can be studied geometrically by looking at the nullcline of z and looking at a folded region, where the orbit jumps from a top segment (in the $\dot{s} > 0$ region) to a bottom segment (in the $\dot{s} < 0$ region) back and forth as shown in Fig. 5. In the singularly perturbed limit ($\varepsilon \rightarrow 0$)

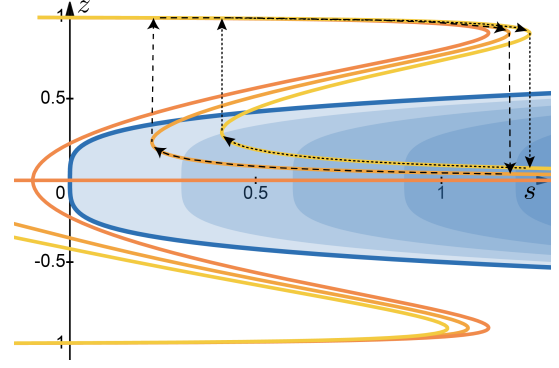


Fig. 5. Nullclines for (1). Three nullclines z for values of b equal to 0 (dark orange), 0.05 (light orange) and 0.1 (yellow). Dashed and dotted lines correspond to spike limit cycle for $b = 0.05$ and $b = 0.1$ respectively, both at the singularly perturbed limit. Blue line is s nullcline. Shaded blue regions correspond to \dot{s} level sets for $-0.3, -0.6, -0.9$ and -1.2 in order of intensity.

we can consider the vertical jumps to be instantaneous, so only the time taken to traverse the top and bottom segments contribute to the period of the oscillation. This implies that as b increases, the width of the segments tends to shrink as the two inflection points of the fold come closer together. Additionally, as the segments slide towards more positive s values the magnitude of \dot{s} increases faster away from the s nullcline (the shaded blue regions become more compressed towards higher s values). These two observations taken together explain why the frequency increases monotonically with b . However, as discussed in Section III, for large enough input values (and these tend to be considerably large in relation to the input threshold) there is always a second Hopf bifurcation where the system saturates, the fixed point becomes stable and the limit cycle disappears. Any application of S-NOD using encoding of input magnitude as spiking frequency will need to consider parameters such that this behavior holds within the relevant input ranges.

The other parameters provide different dials which can also be used to tune the thresholds and other properties of the spiking behavior, such as the amplitude and the duration of individual spikes. In particular, parameter d can tune the amplitude of the spikes, while parameters a , k and k_s can tune the duration and frequency encoding. Even though changes to these parameters are not independent, appropriate simultaneous changes in these can decouple the spike properties and allow for freedom in the design for particular applications. Even though Fig. 2 shows a set of parameters where b^* and z^* are comparable in magnitude to the spike amplitude, these can be designed to be of arbitrary size, such that they are separated by orders of magnitude. This could be important in applications with noisy measurements, where it is important to clearly distinguish sub-threshold and spiking states.

VI. DISCUSSION

The results in this paper show the tractability and robustness of the S-NOD model properties such as input thresholds to

spiking, indecision-breaking and frequency encoding. These properties can be leveraged in order to use S-NOD as a new neuromorphic control block for adaptable robustness and agility in a way that generalizes the approach of [6]. Filtered input, e.g., measurement of the plant output and environment, enters the block as a real-valued signal $b(t)$, and the opinion state $z(t)$ is filtered and transformed into a control signal for the plant that is fed to the actuators. The parameter μ_0 can be adjusted as a function of some aspect of the environment in order to modulate the input threshold, for example in response to urgency or a need for higher responsiveness. S-NOD can be extended to consider multiple agents and/or multiple options similarly to how the NOD model generalizes in [4]. This could allow for rich collective dynamics and for multidimensional opinion spikes enabling more complex actuation.

REFERENCES

- [1] G. Balázsi, A. van Oudenaarden, and J. J. Collins, "Cellular decision making and biological noise: From microbes to mammals," *Cell*, vol. 144, no. 6, p. 910–925, 2011.
- [2] A. M. Hein, "Ecological decision-making: From circuit elements to emerging principles," *Current Opinion in Neurobiology*, vol. 74, p. 102551, 2022.
- [3] V. H. Sridhar, L. Li, D. Gorbonos, M. Nagy, B. R. Schell, T. Sorochkin, N. S. Gov, and I. D. Couzin, "The geometry of decision-making in individuals and collectives," *Proceedings of the National Academy of Sciences*, vol. 118, no. 50, p. e2102157118, 2021.
- [4] A. Bizyaeva, A. Franci, and N. E. Leonard, "Nonlinear opinion dynamics with tunable sensitivity," *IEEE Transactions on Automatic Control*, vol. 68, no. 3, p. 1415–1430, 2023.
- [5] N. E. Leonard, A. Bizyaeva, and A. Franci, "Fast and flexible multiagent decision-making," *Annual Review of Control, Robotics, and Autonomous Systems*, vol. 7, pp. 19–45, 2024.
- [6] C. Cathcart, I. X. Belaustegui, A. Franci, and N. E. Leonard, "Spiking nonlinear opinion dynamics (S-NOD) for agile decision-making," *IEEE Control Systems Letters*, vol. 8, pp. 3267–3272, 2024.
- [7] E. M. Izhikevich, *Dynamical Systems in Neuroscience*. MIT press, 2007.
- [8] J. Guckenheimer and P. Holmes, *Nonlinear Oscillations, Dynamical Systems, and Bifurcations of Vector Fields*. Springer Science & Business Media, 2013, vol. 42.